

## RESULTS FROM KLOE AND DAΦNE\*

FABRIZIO SCURI

on behalf of the KLOE Collaboration<sup>†</sup>

INFN, sezione di Trieste,

Area di Ricerca, Padriciano 99, 34027, Trieste, Italy

e-mail: `fabrizio.scuri@ts.infn.it`*(Received March 29, 2001)*

The status of the KLOE experiment at the DAΦNE facility is presented. The detector on-beam performances are discussed. Methods for the selection and analysis of the relevant  $K_L^0 K_S^0$  decay channels have been developed and optimized with the data collected so far. A summary of preliminary results is given. Analysis of the collected statistics in year 2000 is in progress. The perspectives of the next data taking campaign are also presented.

PACS numbers: 29.40.-n, 11.30.Er, 13.25.Es

---

\* Presented at the Cracow Epiphany Conference on  $b$  Physics and  $CP$  Violation, Cracow, Poland, January 5–7, 2001.

<sup>†</sup> M. Adinolfi, A. Aloisio, F. Ambrosino, A. Andryakov, A. Antonelli, M. Antonelli, F. Anulli, C. Bacci, G. Barbiellini, F. Bellini, G. Bencivenni, S. Bertolucci, C. Bini, C. Bloise, V. Bocci, F. Bossi, P. Branchini, S.A. Bulychjov, G. Cabibbo, A. Calcaterra, R. Caloi, P. Campana, G. Capon, G. Carboni, A. Cardini, M. Casarsa, V. Casavola, G. Cataldi, F. Ceradini, F. Cervelli, F. Cevenini, G. Chiefari, P. Ciambone, S. Conetti, E. De Lucia, G. De Robertis, R. De Sangro, P. De Simone, G. De Zorzi, S. Dell'Agnello, A. Denig, A. Di Domenico, C. Di Donato, S. Di Falco, A. Doria, E. Drago, O. Erriquez, A. Farilla, G. Felici, A. Ferrari, M.L. Ferrer, G. Finocchiaro, C. Forti, A. Franceschi, P. Franzini, M.L. Gao, C. Gatti, P. Gauzzi, A. Giannasi, S. Giovannella, V. Golovatyuk, E. Gorini, F. Grancagnolo, W. Grandegger, E. Graziani, P. Guarnaccia, H.G. Han, S.W. Han, X. Huang, M. Incagli, L. Ingrosso, Y.Y. Jiang, W. Kim, W. Kluge, C. Kuo, V. Kulikov, F. Lacava, G. Lanfranchi, J. Lee-Franzini, T. Lomtadze, C. Luisi, C.S. Mao, M. Martemianov, A. Martini, M. Matyuk, W. Mei, A. Menicucci, L. Merola, R. Messi, S. Miscetti, A. Moalem, S. Moccia, M. Moulson, S. Mueller, F. Murtas, M. Napolitano, A. Nedosekin, M. Panareo, L. Pacciani, P. Pagès, M. Palutan, L. Paoluzzi, E. Pasqualucci, L. Passalacqua, M. Passaseo, A. Passeri, V. Patera, E. Petrolo, G. Petrucci, D. Picca, G. Pirozzi, M. Pollack, L. Pontecorvo, M. Primavera, F. Ruggieri, P. Santangelo, E. Santovetti, G. Saracino, R. D. Schamberger, C. Schwick, B. Sciascia, A. Sciubba, F. Scuri, I. Sfiligoi, J. Shan, P. Silano, T. Spadaro, S. Spagnolo, E. Spiriti, C. Stanescu, G.L. Tong, L. Tortora, E. Valente, P. Valente, B. Valeriani, G. Venanzoni, S. Veneziano, A. Ventura, Y. Wu, Y.G. Xie, P.F. Zema, P.P. Zhao, Y. Zhou.

## 1. Introduction

Since the spring of 1999 the KLOE detector, designed and built for the study of  $CP$  violation in neutral kaons decays, has been recording  $e^+e^-$  collisions at DAΦNE, the  $\phi$ -factory of the Laboratori Nazionali di Frascati (Rome) of INFN.

The KLOE detector was designed to measure  $\text{Re}(\varepsilon'/\varepsilon)$  in one year ( $10^7$  s) with an accuracy of one part in ten thousand, using primarily the double ratio method [1]. For this purpose, at the design luminosity of  $5 \times 10^{32} \text{ cm}^{-2}\text{s}^{-1}$  on the  $\phi$  resonance peak, the DAΦNE collider will deliver as much as  $40 \text{ pb}^{-1}$  per day.

Since  $\sigma(e^+e^- \rightarrow \phi) \sim 3.1 \mu\text{b}$ ,  $\text{B}(\phi \rightarrow K_S^0 K_L^0) = 34.1\%$ , and the  $K_L^0$  decay path is 3.5 m at this energy it follows that for the statistically lowest term of the double ratio measuring  $\text{Re}(\varepsilon'/\varepsilon)$ ,  $\sim 10000 \text{ } K_L^0 \rightarrow \pi^0 \pi^0$  decays per day can be observed by a detector of reasonable dimensions, *i.e.* some 5 m in length and diameter.

Due to severe machine problems, however, at the end of 1999 only  $2.4 \text{ pb}^{-1}$  were collected by KLOE. These data were used mainly to perform studies on the detector performances to assess its capability of observing the relevant  $\phi$  and kaon decay channels, and to start the study of the possible systematics affecting the measurement of  $\varepsilon'/\varepsilon$ .

Many machine problems were understood and solved in the first part of the year 2000, so that more than  $20 \text{ pb}^{-1}$  were collected at the end of that year. Data analysis is in progress and the collected statistics will be used to improve the systematics studies on  $\varepsilon'/\varepsilon$  and to perform accurate measurements of  $\phi$  radiative decays and kaon rare decays.

This paper presents the collider main characteristics, the detector performances and the preliminary results of these analyses in progress.

## 2. The DAΦNE collider

DAΦNE is an electron-positron collider whose c.m. energy is optimized for the  $\phi$  resonance. The design philosophy was based on the possibility to reach the required luminosity of  $5 \times 10^{32} \text{ cm}^{-2}\text{s}^{-1}$  with a moderate single bunch luminosity ( $4 \times 10^{30} \text{ cm}^{-2}\text{s}^{-1}$ , as in the case of the VEPP-2M  $\phi$ -factory in Novosibirsk) and a large number of bunches (120) circulating in the rings. This configuration corresponds to the beam-beam colliding at 5 A/beam, requiring two independent lines.

Two interaction points, the KLOE detector sitting on one of them, are available with a beam crossing angle of 25 mrad; electrons and positrons circulate in coplanar horizontal separate rings with beam crossing frequency of 368.25 Hz and a bunch spacing of 2.7 ns. The bunch sizes at the interaction points are  $20 \mu\text{m}$  in the transverse vertical direction, 2 mm in the transverse

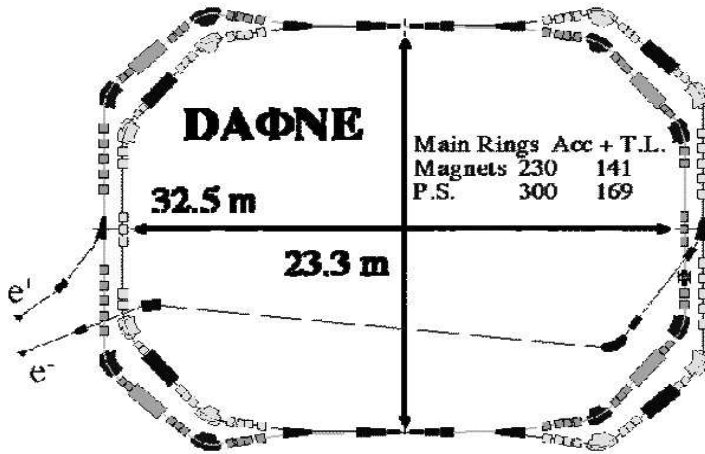


Fig. 1. The DAΦNE collider layout.

horizontal and 13 mm in the longitudinal ones, respectively. The energy spread is about 300 KeV per beam; a schematic layout of DAΦNE is shown in Fig. 1.

### 3. The KLOE detector

The KLOE (KLingExperiment) detector [2] has been designed and built with the primary goal of measuring  $\varepsilon'/\varepsilon$  with a sensitivity of the order of one part in ten thousand.

It consists of a large tracking chamber, a hermetic electromagnetic calorimeter and a large magnet surrounding the whole detector, consisting of a super conducting coil and an iron yoke (see Fig. 2).

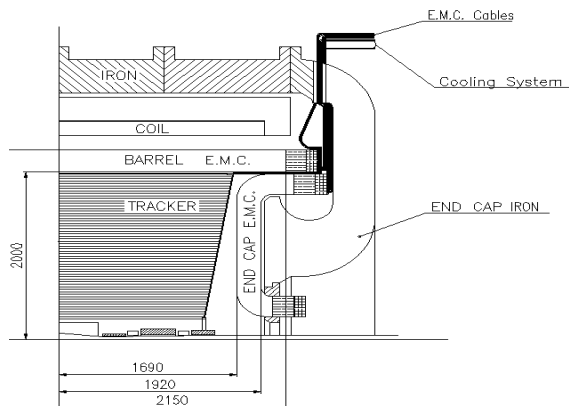


Fig. 2. Side view of the KLOE detector.

The tracking chamber [3] is a cylindrical, 2 m radius, 3.7 m long Drift Chamber (DC). The total number of wires is 52140, out of which 12582 are the sense ones. It operates with a low- $Z$  He gas mixture, to minimize multiple scattering of charged particles and regeneration of  $K_L^0$ 's. The 58 concentric layers of wires are strung in an all-stereo geometry, with constant inward radial displacement at the chamber center. The design resolution on a single measurement is  $\sigma_{r\phi} \leq 200 \mu\text{m}$ , while the  $K_S^0 \rightarrow \pi^+\pi^-$  vertex resolution is  $\sigma_{x,y} \leq 500 \mu\text{m}$ ,  $\sigma_z \leq 1\text{--}2 \text{ mm}$ .

The Electromagnetic Calorimeter (EmC) [4] is a lead-scintillating fibers sampling calorimeter divided into a barrel section and two end caps. The modules of both sections are read-out at the two ends by a total of 4880 photo-multipliers. In order to minimize dead zones in the overlap region between barrel and end caps, the modules of the latter are bent outwards with respect to the decay region; in this way, all photo-multipliers are aligned to the magnet field and the response of the full read-out cell sample can be kept almost uniform.

The calorimeter was designed to detect, with very high efficiency, photons whose energies are as low as 20 MeV, to measure their energy with resolution of  $6\%/\sqrt{E}$  and the time with resolution of  $50 \text{ ps}/\sqrt{E}$  ( $E$  in GeV).

The interaction region is rather unconventional. First, two small calorimeters (QCAL) cover the two sets of low- $\beta$  quadrupoles, which are inside the detector volume, as close as 40 cm from the Interaction Point (IP). Second, the form of the beam pipe is spherical at the IP, with a radius of 10 cm. In this way, the fiducial volume of the  $K_S^0$  decay is fully contained inside the beam pipe and regeneration effects are minimized; moreover, two vertices, close to the source within a few centimetres, can be reconstructed for quantum interferometry measurements. In order to build this pipe a special Aluminum-Beryllium alloy (Albemet) was used.

The trigger strategy depends on both DC and EmC information; a two level scheme [5] has been adopted in order to both produce early triggers with good timing to start the FEE operation and to use as much information as possible from the drift chamber. A valid level 2 signal starts the DAQ system.

The architecture of the latter [6] has been conceived with the purpose of sustaining a throughput of about 40 Mb per second. Data coming from  $\sim 25000$  FEE channels are read-out by 10 independent chains. The 10 sub-pieces of event are then sent to a FDDI GIGA-switch which redirects them to a computer farm where the complete event is reconstructed.

## 4. On-beam detector performances

### 4.1. EmC performances

Absolute calibrations of energy and time scales are performed using collision data. Specifically, a special monitoring task selects Bhabha and  $\gamma\text{--}\gamma$  events; it sets every 100 nb $^{-1}$  the absolute energy and time scales, and performs a cross-calibration of each single calorimeter element. An energy resolution of 5.7%/ $\sqrt{E}$  (GeV) is achieved throughout the whole calorimeter together with a linearity in energy response better than 1% above 80 MeV and 4% between 20 to 80 MeV.

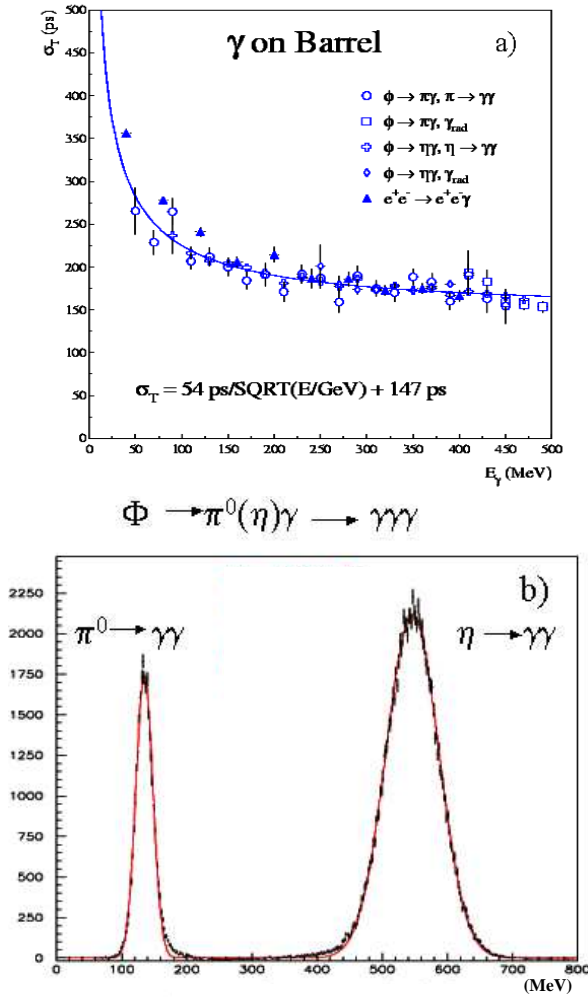


Fig. 3. (a) Calorimeter timing resolution from data; (b)  $\pi^0$  and  $\eta$  reconstructed masses ( $M_{\pi^0} = 135.0$  MeV,  $\sigma_M = 13.0$  MeV,  $M_\eta = 546.4$  MeV,  $\sigma_M = 40.3$  MeV).

Moreover,  $\gamma$  samples from different processes are selected to measure the time resolution at various energies (see Fig. 3(a)); it scales according to the law  $\sigma_T = (54/\sqrt{E(\text{GeV})} \oplus 147)$  ps, where the first term is in agreement with test beam data, while the second (contributed by some miscalibration effects and by the intrinsic time spread due to the bunch length) has to be added in quadrature.

Masses of neutral particles ( $\pi^0$ ,  $\eta$ ) are reconstructed with deviations from the PDG values below 0.6%. In Fig. 3(b) the reconstructed  $\pi^0$  and  $\eta$  masses from the  $\phi$  decay into three photon final state is shown.

#### 4.2. DC performances

Resolutions and residuals of the DC are continuously monitored, cell by cell, making use of Bhabha and  $K_S^0 \rightarrow \pi^+\pi^-$  events; they agree with expectation.

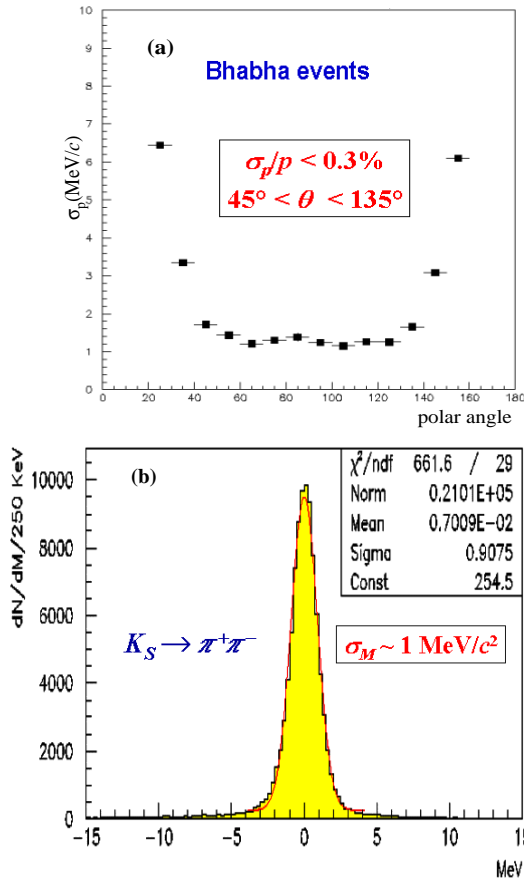


Fig. 4. (a) Momentum resolution as a function of the polar angle for Bhabha events; (b) difference between the  $\pi^+\pi^-$  invariant mass and PDG value of the  $K_S^0$  mass.

The momentum resolution for the 510 MeV/ $c$  electrons and positrons selected from Bhabha scattering events is shown in Fig. 4, as a function of the polar angle of the track; in the region  $50^\circ < \theta < 130^\circ$ , where the projected track length is constant, the resolution is 1.4 MeV/ $c$ , dominated by multiple scattering.

The invariant mass from two unlike sign tracks coming from a vertex within 5 cm from the IP is computed in the  $\pi^+\pi^-$  hypothesis and subtracted from the  $K_S^0$  mass PDG value; the result is shown in Fig. 4(b).  $K_S^0$  decays are well identified: the distribution peaks at the correct value, with a width of 0.9 MeV/ $c^2$ .

Clearly, from these results it follows that the performance of the DC meets well the design specifications.

## 5. Results from the first period of data taking

### 5.1. Neutral kaon physics

When a  $\phi$  meson decays into two neutral kaons,  $C$ -parity invariance forces the two kaons to be in a correlated  $K_S^0$ - $K_L^0$  state. The observation of a  $K_S^0$  therefore, tags the presence of the  $K_L^0$  in the opposite hemisphere and *vice versa*.

Both, in the case of the  $K_L^0$  and in that of the  $K_S^0$ , two different tagging strategies have been developed. Actually, one can select the decays of the  $K_S^0$  into charged or neutral pions to tag  $K_L^0$ 's. Conversely, as a  $K_S^0$  tagging strategy, one can either look for a charged vertex well inside the DC volume, or identify a  $K_L^0$  interacting in the calorimeter with an EmC signal compatible with that of a slowly moving ( $\beta=0.2$ ) neutral particle<sup>1</sup>.

$K_S^0$  decays are tagged according to the prescription described in reference [7]. The tagging procedure is based on two requirements:

1. The presence of a EmC cluster to start the KLOE algorithm used to assign correctly in time all clusters to each  $\phi$  decay.
2. The presence of a EmC cluster in the barrel region with energy larger than 100 MeV and time compatible with that being due to a particle moving with  $\beta = 0.2$ .

The two different types of  $K_S^0$  decays are then selected requiring:

- The presence of four EmC clusters with a timing compatible with the hypothesis of being due to prompt photons (their  $\beta$  must be close to 1, within 5  $\sigma$ 's) to select  $K_S^0 \rightarrow \pi^0\pi^0$  events; other geometrical and kinematical cuts ( $390 \leq M_{4\gamma} \leq 660$  MeV/ $c^2$ ) are applied to reject the background.

---

<sup>1</sup> More than one half of the  $K_L^0$ 's reach the calorimeter before they decay.

- The presence of two oppositely charged tracks originating from the IP, to select  $K_S^0 \rightarrow \pi^+\pi^-$  events. In this second case further requirements are applied to the maximum and the total momentum of the two tracks, to remove the residual background due to charged kaon decays.

Background levels are kept well below 1% for both decays, as shown in reference [7], where the determination of the geometric acceptance, the tagging and selection efficiencies are also discussed. The decay length projected onto the  $K_S^0$  momentum from  $K_S^0 \rightarrow \pi^+\pi^-$  decays are shown in Fig. 5(a) and the 4 photon invariant mass from  $K_S^0 \rightarrow \pi^0\pi^0$  decays in Fig. 5(b).

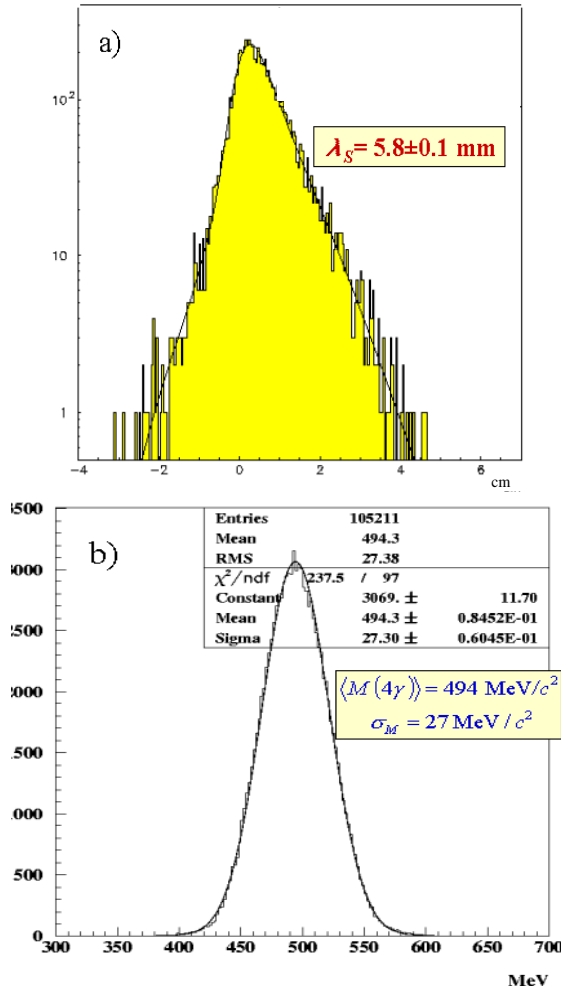


Fig. 5. (a)  $K_S^0$  decay length from  $K_S^0 \rightarrow \pi^+\pi^-$  decays; (b) 4 photon invariant mass from  $K_S^0 \rightarrow \pi^0\pi^0$  decays.



In the 1999 data sample, about 120 000  $K_S^0 \rightarrow \pi^+\pi^-$  and 50 000  $K_S^0 \rightarrow \pi^0\pi^0$  decays have been selected. The latter number sets the statistical accuracy, the first is the most relevant for the study of systematic effects, not finalized yet. The present estimate sets the systematics at the 1% level, a number which can be largely improved by increasing the statistics of the control samples.

With the data sample the following ratio was computed:

$$\frac{\Gamma(K_S^0 \rightarrow \pi^+\pi^-)}{\Gamma(K_S^0 \rightarrow \pi^0\pi^0)} = \frac{N^{+-}}{N^{00}} \frac{\varepsilon_{\text{tag}}^{00}\varepsilon_{\text{rec}}^{00}\varepsilon_{\text{sel}}^{00}\varepsilon_{\text{geo}}^{00}\varepsilon_{\text{trig}}^{00}}{\varepsilon_{\text{tag}}^{+-}\varepsilon_{\text{rec}}^{+-}\varepsilon_{\text{sel}}^{+-}\varepsilon_{\text{geo}}^{+-}\varepsilon_{\text{trig}}^{+-}}, \quad (1)$$

where  $N^{+-}$  ( $N^{00}$ ) is the number of  $K_S^0 \rightarrow \pi^+\pi^-$  ( $K_S^0 \rightarrow \pi^0\pi^0$ ) recorded events and the efficiencies  $\varepsilon$  are quoted with self explaining suffix. Excluding geometric acceptance, which is determined by Monte Carlo simulation, all the relevant efficiencies quoted above are measured using data. This removes the need of reproducing in the Monte Carlo the interactions of hadrons in the calorimeter with high accuracy, a totally untrivial issue at KLOE energies. Also the probability of photon's clusters splitting, particularly relevant in the  $K_S^0 \rightarrow \pi^0\pi^0$  analysis, is determined from data as well as the trigger efficiency, measured by comparing the amount of events when one or two calorimeter trigger sectors were fired. The KLOE result

$$\frac{\text{BR}(K_S^0 \rightarrow \pi^+\pi^-)}{\text{BR}(K_S^0 \rightarrow \pi^0\pi^0)} = 2.237 \pm 0.009 \pm 0.0016$$

is compared with the previous ones in Fig. 6 and with the PDG mean value (grey band). Precision measurements of the ratio in Eq. (1) allow improvement of the accuracy in computing the isospin amplitudes  $A_0$  and  $A_2$  and their phase difference ( $\delta_0 - \delta_2$ ) (normally used to describe the kaon decay into two pions) and inferences on theoretically expected corrections due both to isospin violations in electromagnetic interactions and to inner bremsstrahlung in strong interactions [8].

The cleanest and most copious signature for tagging  $K_L^0$  decays, is the observation of a  $K_S^0 \rightarrow \pi^+\pi^-$  event in the detector. Two oppositely charged tracks originating from a sphere of 6 cm radius about the interaction region, are paired; their invariant mass is computed in the pion hypothesis, and the event is tagged as  $K_S^0 K_L^0$  whenever  $50 < P_{\text{tot}} < 170$  MeV/ $c$  and  $400 < M_{\text{inv}} < 600$  MeV/ $c^2$ .

A search is then performed for either a charged or a neutral vertex along the  $K_L^0$  reconstructed flight direction, to pre-select  $K_L^0 \rightarrow \pi^+\pi^-$  or  $K_L^0 \rightarrow \pi^0\pi^0$  candidates, respectively.

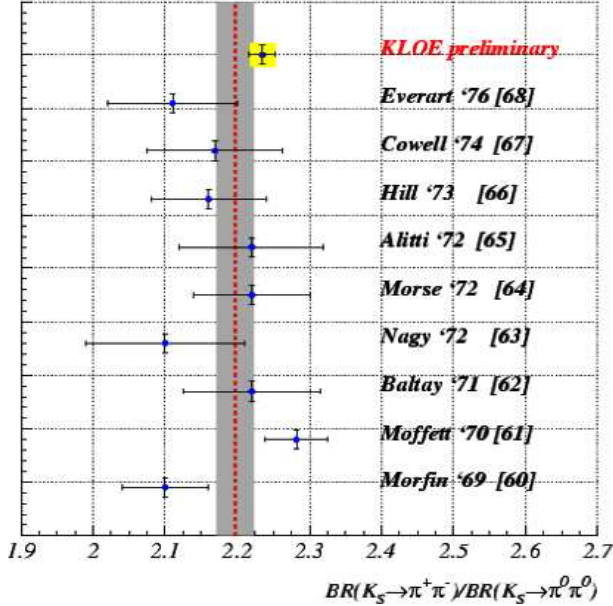


Fig. 6.  $BR(K_S^0 \rightarrow \pi^+ \pi^-) / BR(K_S^0 \rightarrow \pi^0 \pi^0)$  measurement summary.

In the charged case, the missing invariant mass squared and the missing momentum are computed from the charged tracks and the  $K_L^0$  momenta, in the hypothesis that the two tracks belong to pions. The missing momentum is exactly zero for  $\pi^+ \pi^-$  decays and tends to be small for soft neutrino emission in semileptonic decays. The missing invariant mass satisfies  $M_{inv}^2 = M_{\pi^0}^2$  for  $K_L^0 \rightarrow \pi^+ \pi^- \pi^0$  decays, while it is zero for  $\pi^+ \pi^-$  ones (see Fig. 7).

The background for the  $CP$  violating signal, due to the tail of the distribution for  $K_L^0$  semileptonic decays, is strongly suppressed by imposing the missing momentum and the missing squared mass be almost equal to zero. The signal region is identified by the small rectangle in Fig. 7. The invariant mass of the tracks in  $K_L^0 \rightarrow \pi^+ \pi^-$  candidate events is shown in Fig. 8; the statistics refer to the 1999 data sample in which a total 332 candidate events are found with a background contribution estimated by Monte Carlo.

$K_L^0 \rightarrow \pi^0 \pi^0$  decays are observed by selecting neutral vertices with four associated clusters in the calorimeter. Neutral vertices are reconstructed with an algorithm using the timing information of the calorimeter clusters and the  $K_L^0$  momentum direction from the reconstructed  $K_S^0$  one. A loose collinearity cut is then applied between the  $K_L^0$  flight path and the momentum of the  $4\gamma$  system. The final sample is selected requiring the presence of 2 properly reconstructed  $\pi^0$ 's. The statistics refer to a subsample of the full 1999 data sample, corresponding to about  $1 \text{ nb}^{-1}$  of integrated luminos-

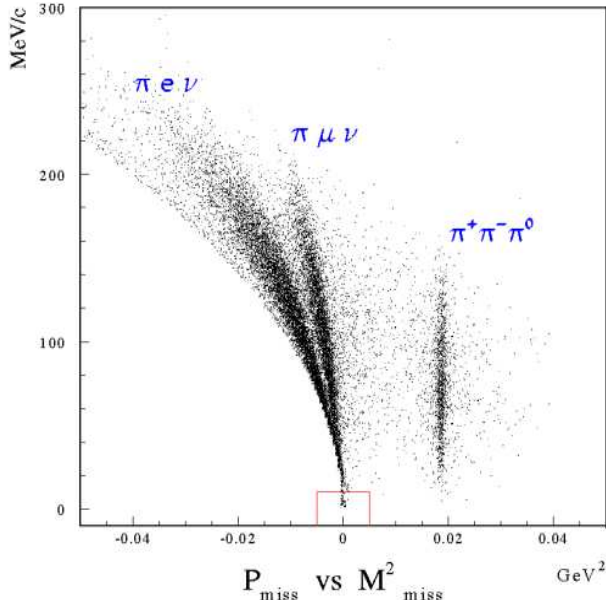


Fig. 7. Separation between various classes of  $K_L^0$  charged decays. The small rectangle bounds the  $CP$  violating signal region.

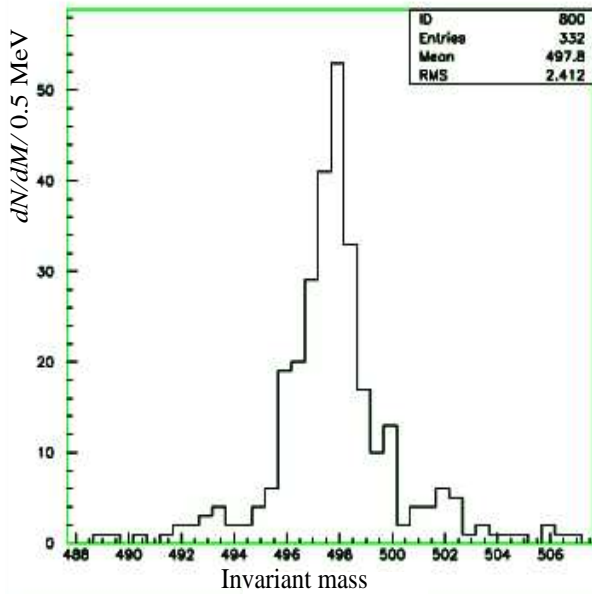


Fig. 8. Measured invariant mass of the two tracks in  $K_L^0 \rightarrow \pi^+ \pi^-$  candidate events.

ity. The invariant mass distribution of this  $2\pi^0$  system is shown in Fig. 9. The contribution to the distribution due to  $K_L^0 \rightarrow \pi^0\pi^0\pi^0$  decays with two lost photons, estimated by Monte Carlo, is shown by the dots in Fig. 9(a); the background subtracted signal is shown in Fig. 9(b). Note that in this analysis no use has been made either of the QCAL information, which might improve the background rejection power up to a factor of 5, or any kinematically constrained fit, which can further enhance the separation between signal and background.

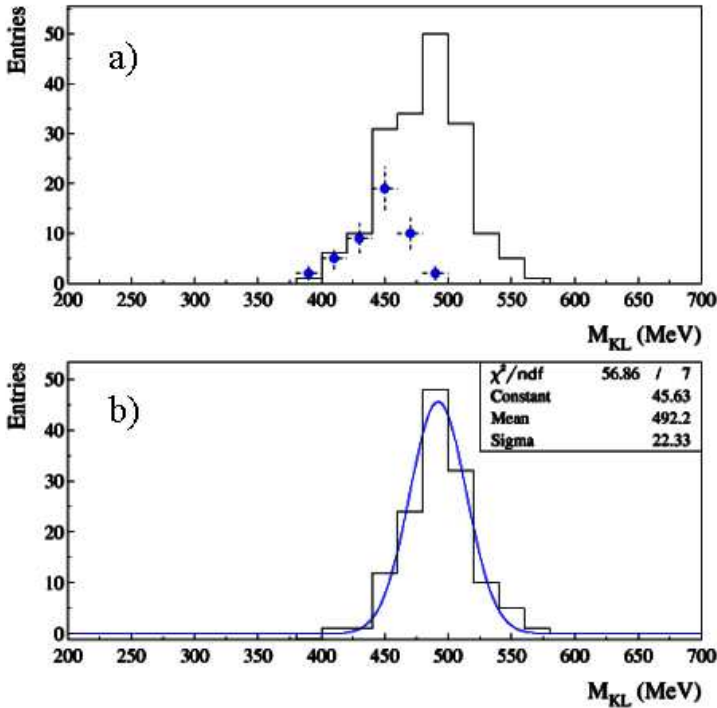


Fig. 9.  $K_L^0$  invariant mass from  $4\gamma$  events; (a) dots represent the Monte Carlo estimated contribution from  $K_L^0 \rightarrow \pi^0\pi^0\pi^0$  decays; (b) background subtracted signal from  $CP$  violating decays.

### 5.2. Non kaonic $\phi$ decays

Preliminary KLOE results on  $\phi$  hadronic decay from the 1999 data taking were presented at the HEP Osaka Conference in Summer 2000 [15]. Cross section and branching ratio values of some rare  $\phi$  radiative decays from the experiments at the DAΦNE and VEPP-2M (Novosibirsk)  $\phi$ -factories are summarized in Table I; all particle secondary decays, branching ratios or their ratios are taken from the PDG 2000 values. Results are at the same accuracy level and are compatible within the errors.

TABLE I

Cross section and branching ratio measurements from experiments at the  $\phi$ -factories; upper error is statistical, lower systematic; <sup>a)</sup> interference with FSR is ignored; <sup>b)</sup> background from  $\rho\pi$  and  $\omega\pi$  decays is estimated by Monte Carlo and subtracted; <sup>c)</sup>  $\text{BR}(\phi \rightarrow \eta'\gamma)$  is normalized to the PDG value of  $\text{BR}(\phi \rightarrow \eta\gamma)$  through the measured ratio between  $\eta$  and  $\eta'$  charged mode decays with three photons in the final state (see reference [15]).

Observed process	KLOE '99	VEPP-2M
$\sigma(e^+e^- \rightarrow \phi) \text{ via } \phi \rightarrow \eta\gamma$	$(3.19_{\pm 0.26}^{\pm 0.02}) \mu\text{b}$	$(3.114_{\pm 0.048}^{\pm 0.034}) \mu\text{b}$ CMD-2 [9]
$\sigma(e^+e^- \rightarrow \omega\pi^0 \rightarrow \pi^0\pi^0\gamma)$	$(0.67_{\pm 0.05}^{\pm 0.04}) \text{nb}$	$(0.74 \pm 0.02) \text{nb}$ SND [10]
$\text{BR}(\phi \rightarrow f_0\gamma \rightarrow \pi^0\pi^0\gamma)$	$(0.81_{\pm 0.06}^{\pm 0.09}) \times 10^{-4}$	$(1.22 \pm 0.12)^{-4}$ SND [11]
$\text{BR}(\phi \rightarrow f_0\gamma \rightarrow \pi^+\pi^-\gamma)$	$\leq 1.6 \times 10^{-4} \text{ }^{\text{a)}} \text{ (90\%C.L.)}$	$(1.93_{\pm 0.50}^{\pm 0.46}) \times 10^{-4}$ CMD-2 [12]
$\text{BR}(\phi \rightarrow a_0\gamma \rightarrow \eta\pi^0\gamma)$	$(0.69_{\pm 0.10}^{\pm 0.14}) \times 10^{-4} \text{ }^{\text{b)}} \text{ (90\%C.L.)}$	$(0.88 \pm 0.17)^{-4}$ SND [11] $(0.49_{\pm 0.06}^{+0.22-0.18})^{-4}$ CMD-2 [13]
$\text{BR}(\phi \rightarrow \eta'\gamma)$	$(0.89_{\pm 0.06}^{\pm 0.20}) \times 10^{-4} \text{ }^{\text{c)}} \text{ (90\%C.L.)}$	$(0.67_{\pm 0.10}^{+0.34-0.29})^{-4}$ SND [14]

KLOE also studied  $\phi$  decays into 3 photon final states obtaining the following result on the ratio between branchings:

$$\frac{\text{BR}(\phi \rightarrow \eta\gamma) \times \text{BR}(\eta \rightarrow \gamma\gamma)}{\text{BR}(\phi \rightarrow \pi^0\gamma)} = 3.85 \pm 0.02 (\text{stat}) \pm 0.12 (\text{sys}). \quad (2)$$

This result is more accurate than the PDG 2000 average of  $(4.05 \pm 0.35)$ .

In the studies on the pseudo-scalars sector, results from  $\eta'$  and  $\eta$  decays were combined and the  $\phi$ - $\omega$  mixing angle  $\theta_V$  taken into account as in the formalism recently proposed by Bramon *et al.* [16]; KLOE obtained the following result for the pseudoscalar mixing angle  $\theta_p$ :

$$\theta_p = \left( -18.9^\circ \text{ }^{+3.6^\circ}_{-2.8^\circ} (\text{stat}) \pm 0.6^\circ (\text{sys}) \right). \quad (3)$$

This result is compared with the theoretical predictions following different estimates in Fig. 10; the vertical band define the  $2\sigma$  area around the KLOE central value.

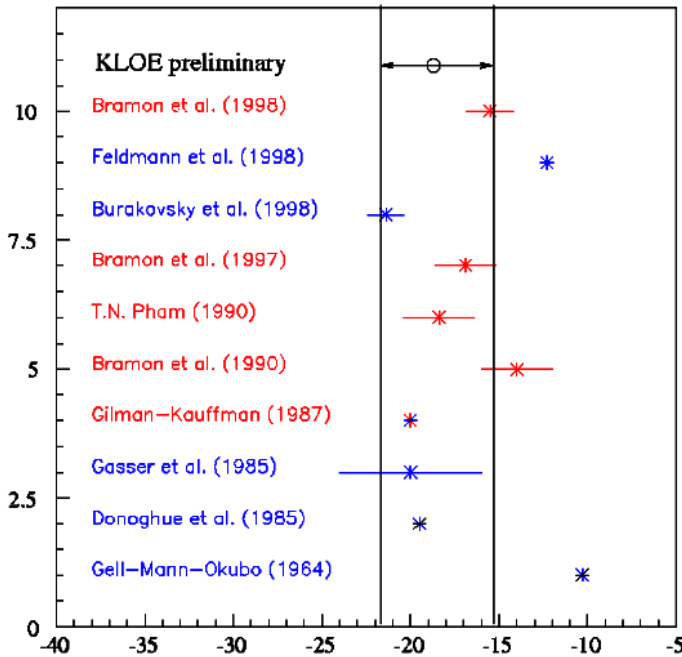


Fig. 10. KLOE preliminary results for the pseudoscalar mixing angle  $\theta_p$  compared with the previous theoretical estimates.

Finally, from the fit of the  $\phi \rightarrow \pi^+ \pi^- \pi^0$  Dalitz-plot as described in reference [15], a new measurement of the  $\rho$  masses,  $m(\rho) = 776.1 \pm 0.1$  MeV,  $\Gamma(\rho) = 145.6 \pm 2.2$  MeV, has been obtained, together with an estimate of the direct decay amplitude relative to the one *via*  $\rho - \pi$  one; all data are in agreement with the PDG values. The KLOE result  $R = A_{\text{direct}}/A_{\rho\pi} = 0.10 \pm 0.01$  represents the first experimental evidence of direct production.

## 7 Perspectives for the future

After some machine hardware upgrade, DAΦNE had restarted operation on April 2000 and had delivered the first stable collisions to KLOE in July. In one month of data taking about  $4 \text{ pb}^{-1}$  were collected. This represented an improvement of a factor 2–3 in delivered luminosity, at the price, however, of an increased background rate. The analysis of these data, together with a joint effort between machine and detector to understand the source of the background, allowed further improvements when machine operation was resumed in autumn 2000 and the goal of about  $1 \text{ pb}^{-1}$  per day was reached by the end of the year.

Analysis of the full data sample of the year 2000 is now in progress; the accumulated statistics should allow KLOE to complete the studies on  $\phi$  radiative decays and to start the study of semi-leptonic and rare kaon decays.

Other machine hardware upgrades are planned for the year 2001 and the achievement of the goal of integrating  $100\text{--}200\text{ pb}^{-1}$  by the end of the year seems likely. When this happens, KLOE could play an important role in the experimental determination of  $\varepsilon'/\varepsilon$  as well as in the rare kaon decay and  $\phi$  radiative decay sectors.

## REFERENCES

- [1] S. Bertolucci *et al.*, *Int. J. Mod. Phys.* **A15S1**, 132 (2000).
- [2] KLOE Collab., A General Purpose Detector for DAΦNE, LNF-92/019.
- [3] KLOE Collab., The KLOE Central Drift Chamber, Addendum to the Technical Proposal, LNF-94/028.
- [4] KLOE Collab., The KLOE Detector, Technical Proposal, LNF-93/002.
- [5] KLOE Collab., The KLOE Trigger System, Addendum to the Technical Proposal, LNF-96/043.
- [6] KLOE Collab., The KLOE Data Acquisition System, Addendum to the Technical Proposal, LNF-95/014.
- [7] G. Cabibbo, PhD Thesis, Universita La Sapienza Roma, 2000.
- [8] J.F. Donoghue *et al.*, *Phys. Lett.* **B192**, 156 (1987); S. Gardner *et al.*, *Phys. Lett.* **B466**, 355 (1999); V. Cirigliano *et al.*, *Phys. Rev.*, **D61**, 093002 (2001).
- [9] R.R. Achmetshin *et al.*, *Phys. Lett.* **B466**, 385 (1999).
- [10] M.V. Achasov *et al.*, *Phys. Lett.* **B486**, 29 (2000).
- [11] M.V. Achasov *et al.*, Recent Results from SND Detector at VEPP-2M, [hep-ex/0010077](#).
- [12] R.R. Achmetshin *et al.*, *Phys. Lett.* **B462**, 371 (1999).
- [13] R.R. Achmetshin *et al.*, *Phys. Lett.* **B494**, 26 (2000).
- [14] V.M. Aulchenko *et al.*, *JETP Lett.* **69**, 97 (1999).
- [15] KLOE Collab., KLOE First Results on Hadronic Physics, [hep-ex/0006036](#).
- [16] A. Bramon *et al.*, *Eur. Phys. J.* **C7**, 271 (1999).